Encoding of brain state changes in local field potentials modulated by motor behaviors

Citation: Stamoulis, Catherine, and Andrew G. Richardson. "Encoding of Brain State Changes in Local Field Potentials Modulated by Motor Behaviors." Journal of Computational Neuroscience 29.3 (2010) : 475-483. © 2010 Springer Science+Business Media.

As Published: http://dx.doi.org/10.1007/s10827-010-0219-6

Publisher: Springer Science + Business Media B.V.

Persistent URL: http://hdl.handle.net/1721.1/65585

Version: Author's final manuscript: final author's manuscript post peer review, without publisher's formatting or copy editing

J Comput Neurosci manuscript No.
(will be inserted by the editor)

Encoding of brain state changes in local field potentials modulated by motor behaviors

Catherine Stamoulis · **Andrew G. Richardson**

Received: July 31, 2009, Revised: November 30, 2009

Abstract Local field potentials (LFPs) measure aggregate neural activity resulting from the coordinated firing of neurons within a local network. We hypothesized that state parameters associated with the underlying brain dynamics may be encoded in LFPs but may not be directly measurable in the signal temporal and spectral contents. Using the Kalman filter we estimated latent state changes in LFPs recorded in monkey motor cortical areas during the execution of a visually instructed reaching task, under different applied force conditions. Prior to the estimation, matched filtering was performed to decouple behavior-relevant signals [24] from unrelated background oscillations. State changes associated with baseline oscillations appeared insignificant. In contrast, state changes estimated from LFP components associated with the execution of movement were significant. Approximately direction-invariant state vectors were consistently observed. Their patterns appeared invariant also to force field conditions, with a peak in the first 200 ms of the movement interval, but exponentially decreasing to the zero state approximately 200 ms from movement onset, also the time at which movement velocity reached its peak. Thus, state appeared to be modulated by the dynamics of movement but neither by movement direction nor by the mechanical environment. Finally, we compared state vectors estimated using the Kalman filter to the basis functions obtained through Principal Component Analysis. The pattern of the estimated state vector was very similar to that of the first PCA component, further suggesting that LFPs may directly encode brain state fluctuations associated with the dynamics of behavior.

Keywords Local Field Potentials · Motor System · State-Space Estimation

PACS 87.19.Lu · 87.19.Ls · 87.85.Ng

Mathematics Subject Classification (2000) 60G35 · 93E10 · 93E11

This work was supported in part by NIH grants 5T32NS048005-05 and 1UL1RR025758-01 (CS) and NS-044393 (AR)

Catherine Stamoulis
Department of Neurology, Harvard Medical School
Beth Israel Deaconess Medical Center
330 Brookline Ave, KS-433
Boston, MA 02215
E-mail: cstamoul@bidmc.harvard.edu

Andrew G. Richardson
MIT, McGovern Institute for Brain Research
Cambridge, MA 02139

1 Introduction

Distinct patterns of aggregate neural activity measured by local field potentials (LFPs) may be associated with distinct, but typically unobserved states of underlying brain dynamics [8][9], i.e, the internal states of the system. Given that LFPs measure localized network activity, these states may not be global such as UP/DOWN but may be local states which undergo region-specific modulation by related behaviors. For example, LFPs recorded in motor cortical areas have been shown to be modulated by dynamic and kinematic aspects of motor behaviors [11][17][4][16][1]. However, LFP signals recorded during these behaviors are still coupled to background oscillations, possibly associated with a global brain state. Thus, during the execution of movement, a related LFP signal may encode both region-specific brain state changes associated with behavior and a behavior-independent, possibly global state encoded in coupled background oscillations in the signal. This often makes the interpretation of LFPs difficult, as it is not clear whether they encode localized aggregate activity of a small neuronal network or global activity of a distributed network [6].

Motor behaviors modulate both the time-domain and frequency domain contents of the LFP signal [11][16][20]. Thus,

related temporal and spectral changes have been specifically associated with distinct states, and their temporal occurrence with state transitions [7][3]. However, beyond these directly estimatable states from the LFP, unobserved (hidden) states may also be encoded in the signal, which may reflect a particular aspect of the underlying dynamics of the network, such as entropy changes or a particular network perturbation. One of the challenges of estimating hidden states and related transitions from the LFP signal is that behavior-induced and background oscillations may be coupled in the signal, making the estimation of global and local network states difficult. We have previously demonstrated that background oscillations may be decoupled from the movement-related signal using *matched filtering*, a quasi-optimum waveform matching technique [24]. In this study we hypothesized that state estimation may be performed separately to movement-related and background LFP signal contributions to identify behavior-modulated and behavior-independent state changes, both encoded in the signal.

State-space or hidden Markov models (HMM) have been proposed to estimate unobserved dynamic changes in the brain and related state transitions [23][7][22]. In this study we assumed that both the observation and latent state processes may be treated to a first approximation as linear and normally distributed and applied the *Kalman filter* [5] to estimate dynamic state from observed LFP signals during the execution of a visually-cued reaching task. Kalman filtering assumes a linear relationship between state variables and measurements, as well as normal distribution of all processes, including the system and measurement noise. There are potential limitations associated with these assumptions. For example, the most appropriate system model may be non-linear, the noise processes may be non-normal and non-white, and the noise statistics may change with time. However, in this study we showed that the linearity assumption is adequate, at least to a first approximation (Figure 3(b)). Also, appropriate transformations of the data, e.g., logarithmic transformation, can be used in general to correct for non-normality, non-linearities, etc, and apply the Kalman filter.

Background oscillations during movement were decoupled from the movement-related signals using matched filtering prior to state estimation. Steady-state (baseline) brain dynamics are present at different task-related intervals and we were interested in estimating corresponding state changes encoded in these signal components. To assess the effect of these oscillations on movement-induced state changes, we also compared state vectors estimated after matched-filtering to corresponding vectors without matched-filtering. All estimations were performed to LFPs recorded under 3 external force conditions, null, clockwise or counterclockwise and washout. Finally, *principal component analysis* (PCA) was also performed, to matrices of all recorded LFPs for each animal and recording site. PCA is typically used to decrease the dimensionality of the data, thus eliminating noisy components. It, therefore, subsequently enables the identification of otherwise hidden data structures or signatures. In particular, the first component accounts for the largest variability of the data. We hypothesized that brain state may be directly encoded in LFPs but may be buried in behavior-induced or unrelated noise, and compared the estimated first signal component obtained from PCA to the state vectors obtained using the Kalman filter.

2 Materials and Methods

2.1 Behavioral Tasks and LFP Preprocessing

The visually-instructed task, data acquisition and data preprocessing have been described in detail in [16]. LFPs were recorded in two male rhesus monkeys, as they performed a large number of trials (typically at least 480) of a learned, visually-cued reaching task divided into four behavioral intervals. Baseline oscillations were recorded during the center-hold period (1s), when the monkeys held a handle in the center of the workspace. This was followed by the instructed delay period, marked by the appearance of the visual cue, directing the animal to move the lever to one of eight directions (at 45^o increments), and the disappearance of the center target. The third interval corresponded to the animal's reaction time between the go signal and movement onset. The fourth interval was the movement time, during which the animal reached the desired target, held the lever at that target and returned to the center-hold position. These task intervals and examples of corresponding LFPs are shown in Figure 1. Both monkeys performed the task with no forces applied to their hand. Monkey A also repeated the task under velocity-dependent clockwise/ counterclockwise curl force fields, which represented novel mechanical environments [16].

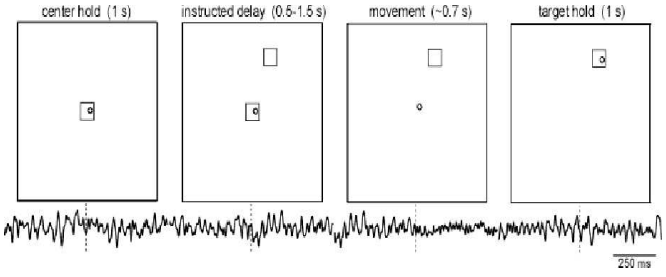

Fig. 1 The behavioral task involved moving a curson (circle), which reflected the endpoint position of a planar manipulandum, between targets (squares) displayed on a monitor. An example raw LFP trace corresponding to each phase of the task is shown below each task interval.

LFPs were recorded from primary motor cortex (M1) and dorsal premotor cortex (PMd), using single tungsten

micro-electrodes positioned with manual micro-drives. Recording locations were changed in each session. Surgical and experimental procedures are described in detail in [16]. All procedures were approved by the Committee on Animal Care at the Massachusetts Institute of Technology. A total of 33 LFPs recorded in the dorsal premotor cortex (PMd) and 48 LFPs recorded in area M1 of monkey A, and 54 LFPs in area M1 of monkey B were analyzed. No LFPs were recorded from PMd of monkey B. All signals were sampled at 2000 Hz and bandpass filtered in the range 1-1000 Hz. Electrode impedance was 0.5-1 MΩ. Power-line noise was attenuated with a stopband filterbank, centered at the 60 Hz harmonics of the noise, in the range 60-480 Hz, with a 3 Hz bandwidth for center frequencies $\leq$ 150 and a 6 Hz bandwidth for center frequencies $>$ 150 Hz. Second order elliptical filters (30 dB attenuation in the stopband, 0.5 dB ripple in the passband) were used. Signals were filtered in both forward and reverse directions to eliminate potential phase distortions due to the non-linear phase of the filter.

Prior to state estimation, LFPs recorded during the delay interval and during movement execution were matched-filtered to decouple the signal contribution associated with the behavior from background oscillations, as described in [24]. The baseline signal recorded during the center-hold interval was used as the template signal (the filter). Following filtering (matching) the template to the coupled delay+background and movement+background signals, respectively, filtered signals represented the best match between the center-hold and delay or movement signals. These were assumed to correspond to background oscillations during these intervals. In contrast, the residual signals from this process were assumed to be the decoupled delay and movement LFPs which were modulated primarily by the motor behavior. Evidently, other processes, such as interval-specific but task unrelated oscillatory activity could also affect the matched-filtered LFPs. However, since they were unknown it was not possible to decouple them from the original signals; only interval-invariant background oscillations were eliminated. Phase corrections were made to account of the non-zero and non-linear phase of the template. Unless otherwise specified, each analyzed LFP represented an average over all trials, recorded during movement in a particular direction. State vector were estimated from these signals. LFPs from areas M1 and PMd in monkey A were not all averaged together. Separate signals were analyzed in the two areas.

2.2 State Estimation

A standard state-space framework was assumed. The underlying brain dynamics encoded in the LFP signals were assumed to result from a continuous, linear Gaussian process described by a set of state and observation equations, respectively, with zero input:

$$\mathbf{x}(t) = \mathbf{A}\mathbf{x}(t-1) + v(t) \quad (1)$$

$$\mathbf{y}(t) = \mathbf{C}\mathbf{x}(t) + \mathbf{w}(t) \quad (2)$$

where $\mathbf{x}(t) \in \mathbb{R}^p$ is the state vector, assuming the system has p states. Here it was assumed that each direction of movement represents a separate state and thus at least 8 distinct states could be estimated from the data, i.e., $p = 8$. Thus the *state transition* matrix $\mathbf{A}$ was assumed to be an $8X8$ matrix. The observed signals $\mathbf{y}(t) \in \mathbb{R}^n$, where $n = no_{sessions} \times no_{directions}$ corresponded to the trial-averaged LFPs at each direction of movement, at time t, e.g., for each of the 33 recording sessions from PMd, 8 LFPs were ultimately analyzed, each averaged over all trials in a particular direction. In that case, $n = 264$, and similarly for the 48 sessions in M1 for monkey A, $n = 384$ and for 54 sessions for monkey B, $n = 432$. Thus, the *observation matrix* $\mathbf{C}$ was assumed to be an $nX8$ matrix. We also estimated state vectors for each recording session, with $vecy(t)$ corresponding to trial-averaged LFPs, i.e., with $n = 8$, to establish confidence bands for the estimates. Both the state vector $\mathbf{x}(t)$ and observed signal $\mathbf{y}(t)$ were both assumed to be random processes. System and measurement noise terms $v(t)$ and $\mathbf{w}(t)$ were assumed to be independent, identically distributed, zero-mean Gaussian processes with covariances Q and R, respectively, which are typically unknown. Dynamic 'state' may refer to different latent variables. Although we initially assumed that a distinct state was associated with each direction of movement when setting the order of the model, we showed in the analysis that in fact the number of distinct states was significantly smaller (possibly 1), and thus the estimated state vector that may be independent of movement direction. Nevertheless, this initial assumption enabled us to investigate the invariance (or lack of) of the state vector with respect to the kinematics of the behavior, as described in Section 3. Parameters $\theta = \{A, C, Q, R\}$ are typically estimated by maximizing their log-likelihood $\mathscr{L}(\theta)$, through either gradient-based maximum-likelihood methods, or the expectation-maximization (EM) algorithm [15].

To demonstrate that estimated states are not simply mathematical constructs but represent true, and in this study unobserved, characteristics of the data, consider the following simple example: a simulated random time series modulated by a step function, resulting in the sequence shown in Figure 2 (top plot). Suppose we want to estimate the corresponding state vector, assuming a two-state system model. Using the state-space representation in Equations 1-2 with the order of the system $n = 2$, we estimated two states, both step functions with different amplitudes. One state vector is shown in the bottom plot of Figure 2. In this example, the step-like state although assumed to be unobservable, is visually

distinguishable in the output signal and thus a direct comparison with the estimated vectors can be made.

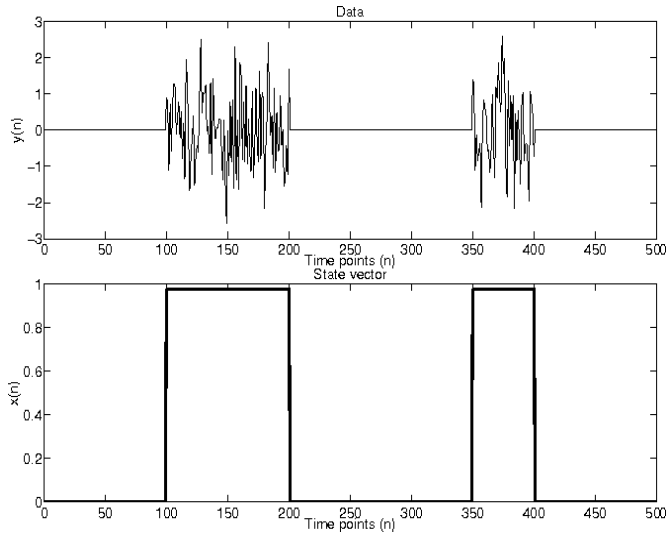

Fig. 2 Measured system output (top plot) and corresponding state vector (bottom plot) obtained using the Kalman filter.

In this study all parameters were estimated using the EM algorithm [2]. They were updated at each step (the E-step of the EM algorithm) and the expected log-likelihood was maximized with respect to these parameters (the M-step). The process was repeated until convergence. We initialized the parameters as follows: for each LFP, the initial state $x(0)$ was assumed to be zero, and the state covariance matrix was also assumed to be a zero-matrix. The measurement covariance matrix was assumed to be a diagonal matrix of the signal variances, i.e, $R = diag(\sigma_i^2)$, $i = 1, \cdots, n$. Figure 3(a) summarizes the effect of varying the initial conditions (initial state vector and associated covariance matrix), on the estimated state-vectors in behavior-relevant task intervals. Figure 3(b) assesses the accuracy of the linear model and estimated parameters by comparing quantiles of measured and model-predicted data (Kolmogorov-Smirnov (K-S) plots). Variation of the initialization of the parameters did not result in significant changes in the state vector signature, but predominantly in temporally localized variability of state amplitude (as shown by the vector bounds in in Figure 3(a)). Based on the K-S goodness of fit plots and corresponding confidence intervals, the model-predicted data completely lies within the 95% confidence bounds and thus the linear state model appears to adequately describe the system, at least to a first approximation.

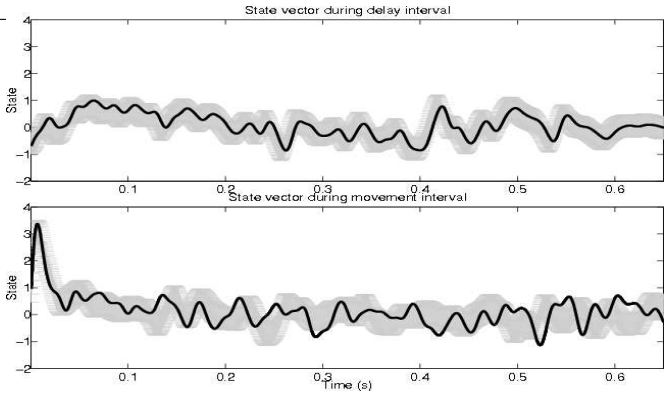

(a) Variation in state estimates due to initial conditions.

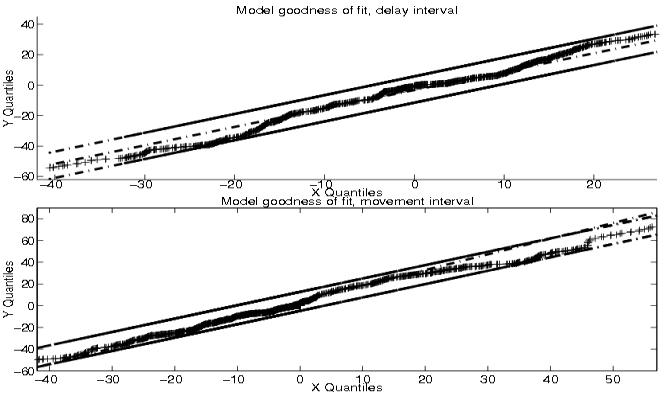

(b) Model fit and confidence intervals.

Fig. 3 Top plot: state estimates for the delay (top) and movement (bottom) intervals and corresponding range of variability (shaded area) when initial estimates are varied, for one direction of movement. Bottom plot: quantile plots for the delay (top) and movement(bottom) intervals. From the estimated parameters and the state vector, model-based LFP amplitudes may be predicted and compared to the true measurements. Solid straight lines correspond to estimated confidence intervals. The dashed line corresponds to the Gaussian distribution.

3 Analysis

Raw and matched-filtered LFPs, recorded during the execution of the motor task, in all directions of movements and under all applied force field conditions (null, forces, washout) were analyzed. We examined state vectors corresponding to different task-related intervals, particularly the instructed delay and movement execution. In a previous study [24] we have shown that application of a linear, waveform-matching filter (the *matched-filter*) to the LFP signal during these intervals enables the decoupling of behavior-related signal contributions to the LFP from unrelated background oscillations. State vectors corresponding to these oscillations may be associated with an inherent property of the network or a global state, whereas state vectors associated with the signal component modulated by the behavior may correspond to region-specific and behavior-specific state changes. We, therefore, applied matched-filtering to raw LFPs, as described in [24] and compared state vectors estimated from the raw and filtered signals, respectively. In regard to the background oscillations, we first estimated state vectors corresponding to the directly measured center-hold signal. We then used this signal as the template in matched-filtering to decouple back-

ground oscillations during the delay interval and estimated the state vector corresponding to these oscillations. We repeated this process for both the reaction and movement intervals. Figure 4 shows an example of the variation of LFP background oscillations (for one LFP, averaged over all trials for a particular direction of movement) during the entire task and corresponding state vector. Inter-trial state fluctuations are superimposed. The LFP signature (or at least its envelope) is preserved in the state vector, particularly during the movement interval and to a lesser extent during the delay interval, which indicates the adequacy of the linear model. The frequency content of background oscillations appears to be slightly modulated during the task, particularly during the delay interval, where low-amplitude, higher frequency signal contributions appear. However, corresponding state fluctuations around the zero state appear insignificant during the entire duration of the task, and are assumed to correspond to the background steady (or equilibrium) state. There are more rapid fluctuations of state during the delay and movement intervals, possibly corresponding to the behavior-induced perturbation to the system. The delay interval has been associated with motor planning [18][4]. Thus, although behavior-independent state changes appear to be insignificant during the task, there is increased state 'noise' in the system.

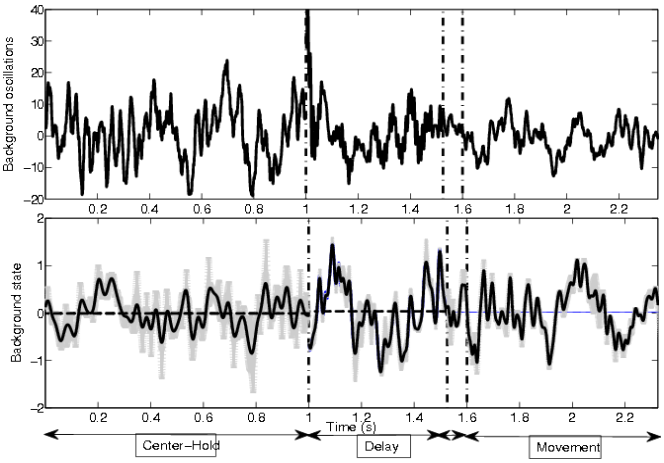

Fig. 4 Example of the variation of background oscillations, directly measured during the center-hold interval and estimated during all other intervals via matched-filtering of corresponding LFP signals (averaged over all trials). The inter-LFP variability of the background state vector (lower plot) is superimposed (gray region).

We also examined state vectors corresponding to decoupled, behaviorally-modulated signal components during the delay and movement intervals. Examples, are shown in Figures 5 and 6, respectively.

Note that matched filtering facilitated the estimation of a state vector with a specific signature rather than a random vector as shown in the left bottom panel of Figure 5, corresponding to the state of the unfiltered delay signal.

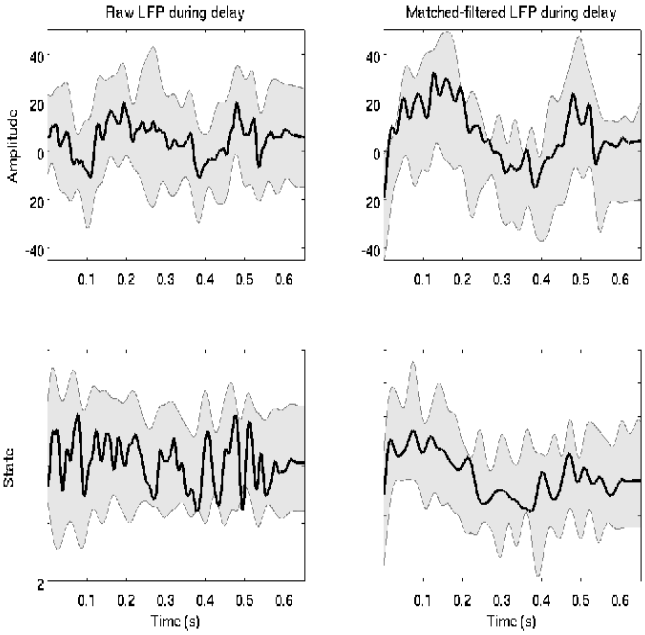

Fig. 5 Raw and matched-filtered LFPs (averaged over all trials and LFPs for a single direction of movement) and corresponding state vectors for the delay interval.

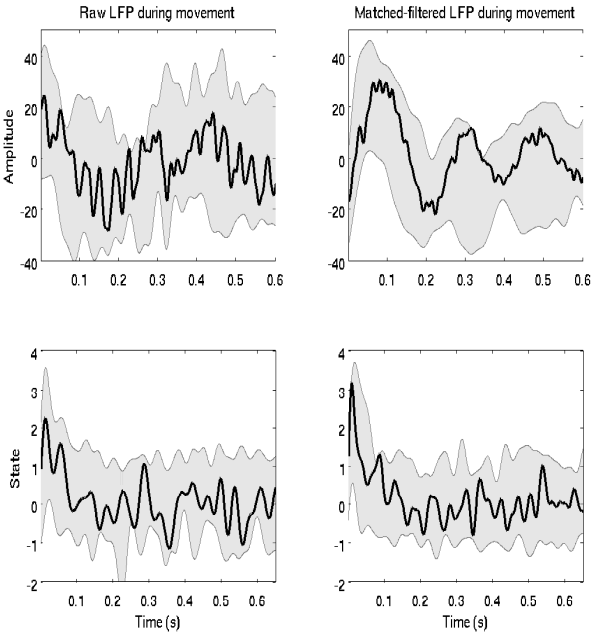

Fig. 6 Raw and matched-filtered LFPs and state vectors for the movement interval. LFPs correspond to a single direction of movement (112.5^o) and the inter-trial variability is superimposed to the averaged signal and state vector.

Similarly to the delay signal, matched-filtering increased the signal-to-noise ratio and thus enabled the estimation of a specific state vector signature during movement execution, and decreased the inter-trial variability of that vector. Note that during the execution of movement a peak state is reached in the first 100 ms of movement and exponentially decreases to the zero state at approximately 200 ms from movement

onset. This is also the time of minimum LFP amplitude, as shown for example in the right top panel of Figure 6 and the time of maximum velocity of movement [16][24]. Therefore, it appears that the first 200 ms of movement correspond to the time of predominant perturbation of brain dynamics, at least in local brain networks of motor cortical regions. Following this system perturbation due to the behavior, the dynamics rapidly return to the steady state (from state 4 to 0). To ensure that this state variation was not an artifact due to the segmentation of the interval, we recomputed state independently for different segments of movement and consistently estimated a similar pattern. In contrast, there is no clear state vector signature in the delay interval and state fluctuates in the range [-1,1], similarly to that of background oscillations. However, the state vector signature is not entirely random. It appears to have a similar envelope as the measured LFPs. In contrast, the state vector during movement execution has a different waveform than the corresponding LFP. Note that [22] report similar state signatures, estimated from spike trains. In that study increased state was directly related to increased firing rate. In this study, single cell recordings were also made (the same recordings were filtered in two different ways to obtain single cell activity and LFPs), and increased firing rate at movement onset was also observed [16]. This suggests that the latent state encoded in the LFP may be directly related to the firing rate of individual neurons, the aggregate activity of which constitutes the LFP signal.

We also examined state variation as a function of applied forces. Previous studies have shown that LFPs are modulated by novel mechanical environments [16]. The force field applied to the animal's hand represents an additional (external) perturbation to the system. Examples of estimated state vectors, averaged over all trials and LFPs in each direction of movement, for the three force conditions during the delay and movement intervals, are shown in Figures 7(a)-7(b).

State vector signatures during the two intervals did not appear to be modulated by external forces. State varied quasi-randomly during the delay interval and exponentially decayed during the movement interval, independently of force conditions. Under null force conditions the animals performed a learned task and thus their hand path trajectories were approximately straight lines. The application of forces caused these paths to become curved due to the novel mechanical environment. With increasing number of trials, the animals adapted to the task and this adaptation was reflected in the progressively straighter hand trajectories. During the washout trials, the animals de-adapted to the force conditions and re-adapted to the null conditions. [16] reported significant de-adaptation during the washout trials, based on the hand trajectories, which were curved in opposite directions than those during force application. For some directions of movement, such as that shown in Figure 7(b) (but not all),

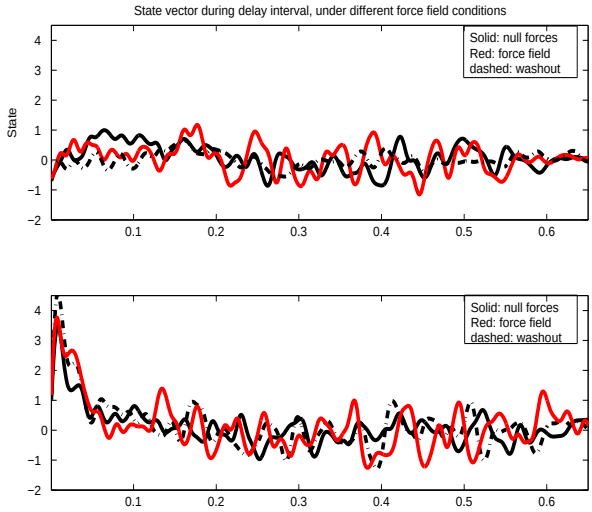

(a) Example of state variation with applied forces during the delay (top plot) and movement intervals (bottom plot), averaged over all relevant trials, for one direction of movement (22.5^o).

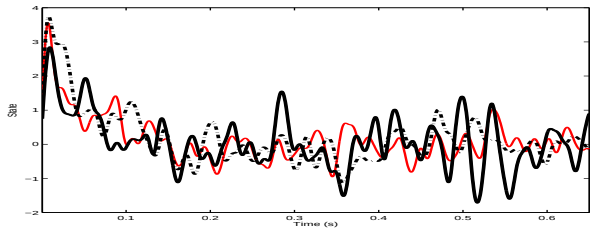

(b) State variation during movement for another direction of movement (292.5^o).

Fig. 7 Solid black corresponds to null forces, red to clockwise or counterclockwise forces, and dashed to washout.

initial state amplitude appeared to increase both during the force and washout trials (in this example the maximum state is $\sim$3 under null conditions and $\sim$ 4 for clockwise forces and washout conditions) possibly reflecting the increased system perturbations, as well as adaptation and de-adaptation to the mechanical environment [16].

Finally, we examined state as a function of direction of movement, i.e., we compared the 8 state vectors estimated from the entire dataset, instead of those obtained from each trial-averaged LFP. In Figure 8 these state vectors are superimposed. In addition, we applied PCA to matrices of all trial-averaged LFPs and examined corresponding principal components, i.e., PCA was performed on matrices of size nXm, where m is the interval length $n = no_{LFPs} \times 8$, with no_{LFPs} corresponding to the number of recording sessions. PCA may be applied to estimate hidden data structures, through reduction in data dimensionality and thus elimination of noise-related components. Here at most 4-5 principal components were estimated from the data. In Figure 8, the first principal component (red line) is superimposed to the state vectors. In general, this component accounts for most of the variability of the data. State vectors for the delay interval are shown in the top plot, and corresponding vectors

for the movement interval, are shown the bottom plot, both under null force conditions.

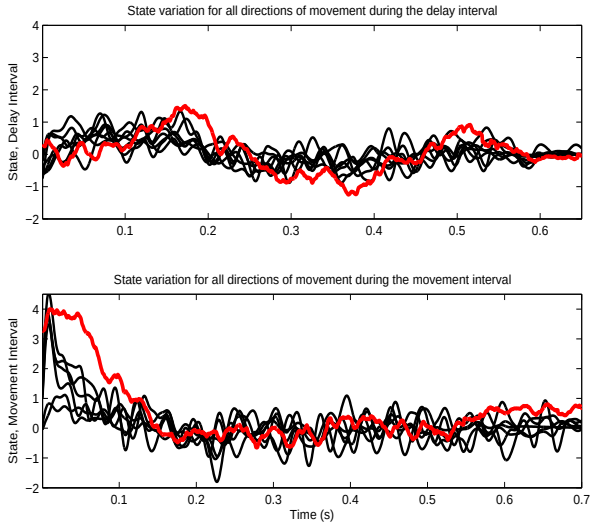

Fig. 8 Example of the variation of background oscillations, measured during the center-hold interval and estimated, using matched-filtering,from the LFP signal during all task-related intervals (averaged over all trials).

Temporal variability of state during the movement interval appeared invariant to movement direction for 6 of the eight directions. Interestingly, for two directions of movement (67.5^o and 247.5^o), the initial state was significantly lower. Overall, an initial increase in state in the first 100 ms was followed by exponential delay back to steady-state and subsequent small fluctuations around that state for the remaining interval. These signatures are similar to movement velocity curves observed by [16]. Therefore, it appears that at least the 'state' encoded in the LFP estimated via the Kalman filter and corresponding to the first principal component, reflects the dynamics of movement. In addition, we observed that the signature of the first principal component was similar to the estimated state vector patterns. This further indicates that state may be directly encoded in the LFP, may not be directly observable due to interfering processes, possibly unrelated to the behavior, but may be recoverable by different estimation methods.

4 Discussion

Local field potentials are modulated by behavior and have been shown to encode both propertied of local networks and global aspects of brain dynamics. However, interfering processes such as background oscillations and other unrelated to the behavior processes also contribute to LFP signals. Thus, intrinsic network dynamics and transient state changes induced by the behavior may be hidden and thus appear unobservable. We have used a linear model to describe the relationship between brain state and measured LFP signal and have estimated the temporal evolution of states during the execution of a reaching task, for different movement directions and force conditions. Signal contributions associated with background oscillations and movement-related LFP components were decoupled using matched-filtering. State was then estimated separately, assuming the two components reflected different brain dynamics, i.e., behavior-dependent localized dynamics versus behavior-independent, possibly global and/or equilibrium dynamics. We were unable to test the global nature of the estimated background state, since we did not simultaneously record LFPs from different brain regions, but were able to estimate distinct state vectors associated with background oscillations, which varied insignificantly during the entire duration of the task, and state vectors that were specifically modulated by the dynamics of the behavior. Background state fluctuated randomly in the range [-1,1], possibly reflecting steady-state or network equilibrium. During the instructed delay interval which has been implicated in motor planning, state also fluctuated quasi-randomly in the same range. However, its waveform (or envelope of) showed similarities to the actual LFP waveform. This was observed in LFPs recorded in both M1 and PMd. Significant state changes were estimated only during movement and only in M1 of both animals. Specifically, an initial increase in state at movement onset was consistently estimated, possibly reflecting the increased firing rate of individual neurons reported in [16] during the same experimental studies described here. In turn, this implies that characteristics of the dynamics of individual neurons may be encoded in the LFP signal but may be unobservable. State exponentially decayed in the first 200 ms of movement and rapidly returned to the zero state with insignificant fluctuations in the range [-1,1] in the remaining movement interval. A peak in LFP amplitude in the first 200 ms and corresponding peak in movement velocity has been previously reported [16][24]. The state vector during movement appeared invariant to most movement directions. Although the assumed state model initially allowed the estimation distinct state vectors corresponding to each direction of movement, there was a remarkable similarity in the termporal patterns of these vectors. In addition, for a few directions initial state at movement onset was higher during force and washout trials than during corresponding null trials, possibly reflecting adaptation to the novel mechanical environment under force conditions, and subsequent de-adaptation during washout. Overall, the state vector signature was remarkably robust to both force conditions and movement direction. The estimated state parameter cannot solely reflect the movement/no movement states, since the animals continued moving after the first 200 ms, and returned to the center hold

position. Instead, it may reflect the perturbation of the system which is abrupt and maximum at movement onset, and decreases to a new equilibrium state as the animal reaches the target position. The return to the center-hold position may represent a smaller perturbation. Finally, the estimated state vector pattern was similar to the first principal component of the data obtained via PCA. This implies that dynamic state may be directly encoded in the LFP signal but may be hidden due to interfering processes, represented by distinct principal components. Once these are decomposed, the 'state' component may be identified. Interestingly, despite matched-filtering which eliminated at least the contribution of background oscillations, the state vector waveform was still not directly observable in the filtered LFP signal, indicating that there may be additional processes coupled to the behavior-related component. The patterns of estimated state vectors were consistent only in LFPs recorded from area M1 of both monkeys. State vectors from LFPs in PMd varied significantly among LFPs. Only about 20% had similar patterns as those in M1. The lack of state vector similarity in the two areas may in part be due to the visuo-motor dependency of neurons in PMd, and/or the distance of the recording site from M1. In summary, our results demonstrate that the LFP signal encodes dynamic aspects of behavior, unrelated background dynamics with distinct state fluctuations, and possibly the dynamics of individual neurons, particularly the modulation of their firing rate by the motor behavior.

References

1. Baker, S.N., Kilner, J.M., Pinches, E.M., Lemon, R.N., The Role of Synchrony and Oscillations in the Motor Output, *Experimental Brain Research*, 128: 109-117, 1999.
2. Dempster, A.P., Laird, N.M., Rubin, D.B., Maximum Likelihood from Incomplete Data via th EM Algorithm, *Journal of the Royal Statistical Society*, Series B, 39(1):1-38, 1977.
3. Garvasoni, D., Lin, S.C., Ribieiro, S., Soares, E.S., Pantoja, J., Nicolelis, M.A.L., Global Forebrain Dynamics Predict Rat Behavioral States and their Transitions, *J. Neurosci.*, 24(49):11137-11147, 2004.
4. Hatsopoulos, N.G., et al., Decoding Continuous and Discrete Motor Behaviors Using Motor and Premotor Cortical Ensembles, *J. Neurophysiol.*, 96: 1658-1663, 2006.
5. Kalman, R.E., A New Approach to Linear Filtering and Prediction Problems, *Transactions of the ASME - Journal of Basic Engineering*, 82, Series D, 35-45, 1960.
6. Katzner, S., Nauhaus, I., Benucci, A., Bonin, V., Ringach, D.L., Carandini, M., Local Origin of Field Potentials in Visual Cortex, *Neuron*, 61:35-41, 2009.
7. Kemere, C., Santhanam, G. Yu, B.M., Afshar, A., Ryu, S.I., Meng, T.H., Shenoy, K.V., Detecting Neural-State Transitions Using Hidden Markov Models for Motor Cortical Prostheses, *J. Neurophysiol.*, 100:2441-2452, 2008.
8. Lin, S.C., Gervasoni, D., Defining Global Brain States Using Multi-Electrode Field Potential Recordings, *Frontiers in Neuroscience: Methods for Neural Ensemble Recordings'*, Ch. 8, Nicolelis, M. Editor, CRC Press, 2008.
9. Lopes da Silva, F.H., Neural Mechanisms Underlying Brain Waves: From Neural Membranes to Networks, *Electroencephal. Clin. Neurophysiol.*, 79:81-93, 1991.
10. Murthy, V.N, Fetz, E.E., Coherent 25- to 35-Hz Oscillations in the Sensorimotor Cortex of Awake Behaving Monkeys, *Proc. Natl. Acad. Sci.*, 89:5670-5674, 1992.
11. Murthy, V.N, Fetz, E.E., Oscillatory Activity in Sensorimotor Contex of Awake Monkeys: Synchronization of Local Field Potentials and Relation to Behavior, *J. Neurophysiol.*, 76(6):3849-3967, 1996.
12. Murthy, V.N, Fetz, E.E., Coherent 25- to 35-Hz Oscillations in the Sensorimotor Cortex of Awake Behaving Monkeys, *Proc. Natl. Acad. Sci.*, 89:5670-5674, 1992.
13. Nicolelis, M., Baccala, L.A., Lin, C.S., Chapin, J.K., Sensorimotor Encoding by Synchronous Neural Ensemble Activity at Multiple Levels of the Somatosensory System, *Science*, 268(5215):1353-1358, 1995.
14. O'Leary, J., Hatsopoulos, N., Early Visuomotor Representations Revealed from Evoked Local Field Potentials in Motor and Premotor Cortical Areas, *J. Neurophysiol.* 96: 1492-1506, 2006.
15. Olsson, R.K., Petersen, K.B., Lehn-Schioler, T., State-Space Models: from the EM Algorithm to a Gradient Approach, *Neural Computation*, 19:1097-1111, 2007.
16. Richardson, A.G., Role of the Precentral Cortex in Adapting Behavior to Different Mechanical Environments, Ph.D thesis, Massachusetts Institute of Technology, 2007.
17. Rickert, J., et al., Encoding of Movement Direction in Different Frequency Ranges of Motor Cortical Local Field Potentials, *J. Neurosci.*, 25(3): 8815-8824, 2005.
18. Roux, S., et al., The pre-movement component of motor cortical local field potentials reflects the level of expectancy,*Behav Brain Res.* 169: 335-351, 2006.
19. Rubino, D., Robins, K.A., Hatsopoulos, N.G., Propagating waves mediate information transfer in the motor cortex, *Nature Neurosci.*, Vol. 9, No. 12, 1549-1557, 2006.
20. Sanes, J.N., Donoghue, J.P., Oscillations in local field potentials of the primate motor cortex during voluntary movement, *Proc. Natl. Acad. Sci. USA*, Vol. 90, pp. 4470-4474, 1993.
21. Sirota, A., Montgomery, S., Isomura, Y., Zugaro, M. Buzsaki, G., Entrainment of Neocortical Neurons and Gamma Oscillations by the Hippocampal Theta Rhythm, *Neuron*, Vol. 60. No. 4, 683-697, 2008.
22. Smith, A.C., Brown, E.N., Estimating a State-Space Model from Point Process Observations, *Neural Computation*, 15:965-991, 2003.
23. Srinivasan, L., Eden, U., Mitter, S.K., Brown, E.N., General-Purpose Filter Design for Neural Prosthetic Devices,
24. Stamoulis, C., Richardson, A.G., Application of matched filtering to identify behavioral modulation of brain oscillations, *J. Comp. Neurosci.*, 2009 (in press).
25. Van Trees, H.L., Detection, Estimation and Modulation Theory, John Wiley & Sons, 2003.